

OPINION

ESKAPEing the labyrinth of antibacterial discovery

Ruben Tommasi, Dean G. Brown, Grant K. Walkup, John I. Manchester and Alita A. Miller

Abstract | Antimicrobial drug resistance is a growing threat to global public health. Multidrug resistance among the 'ESKAPE' organisms — encompassing *Enterococcus faecium*, *Staphylococcus aureus*, *Klebsiella pneumoniae*, *Acinetobacter baumannii*, *Pseudomonas aeruginosa* and *Enterobacter* spp. — is of particular concern because they are responsible for many serious infections in hospitals. Although some promising agents are in the pipeline, there is an urgent need for new antibiotic scaffolds. However, antibacterial researchers have struggled to identify new small molecules with meaningful cellular activity, especially those effective against multidrug-resistant Gram-negative pathogens. This difficulty ultimately stems from an incomplete understanding of efflux systems and compound permeation through bacterial membranes. This Opinion article describes findings from target-based and phenotypic screening efforts carried out at AstraZeneca over the past decade, discusses some of the subsequent chemistry challenges and concludes with a description of new approaches comprising a combination of computational modelling and advanced biological tools which may pave the way towards the discovery of new antibacterial agents.

Despite the real and growing public health threat posed by antibiotic resistance¹, pharmaceutical companies continue to divest from antibacterial research. The reasons for this divestment are partly technical, as replacing historically useful broad-spectrum agents with new drugs with similar spectra has proven to be extremely challenging, and partly economic, as antibiotics have a poor projected return on investment. As a result, the overall private sector investment in new antibacterial agents is below critical funding levels².

Although the incredibly urgent need for novel antibacterial therapies seems to have finally forced the regulatory landscape to accept more focused and less costly clinical trials³, conventional drug discovery approaches (for example, target-based or phenotypic high-throughput screening (HTS)) have not worked in this therapeutic area⁴. A Review by Payne

*et al.*⁴ that described the challenges at GlaxoSmithKline (GSK) in identifying promising new leads for genetically validated antibacterial targets illustrated this conundrum: between 1995 and 2001, an extensive evaluation of hundreds of potential targets and 70 primarily biochemical HTS campaigns were performed. Despite this, few progressable leads were identified, and none of these could be elaborated into development candidates. In the majority of the screening campaigns no hits were identified. As a result, one of the recommendations of these authors was to shift efforts towards chemically diverse libraries as sources of new antibacterials⁴.

The divergent physicochemical property profiles of antibacterials have also been published⁵. The size and hydrophobicity of a set of 147 antibacterials, which are either on the market or in clinical trials, were compared to a set of 4,623 drugs that lack antibacterial

properties, and broad-spectrum antibacterial agents were found to be substantially more polar than other drugs. Compounds with the particular molecular weights, LogD values and polar surface areas of antibacterials are typically not well-represented in corporate screening collections designed to target human proteins.

Nevertheless, although screening more diverse collections may well be valuable, in our experience it is not sufficient to improve the success rates of traditional antibacterial drug discovery projects. Here, we first present the results from AstraZeneca's antibacterial discovery efforts between 2001 and 2010, which illustrate that hit identification was not the main challenge in our target-driven drug discovery programmes. Instead, the process of converting inhibitors of purified target enzymes into compounds with whole-cell activity was the most frequent point of attrition in our antibacterial screening efforts — a challenge that has been impeded in most part by a lack of understanding of the rules governing cell penetration. We also discuss novel approaches that are emerging to address these challenges, including how our understanding of bacterial permeability can be improved through the combined use of genomics and computational modelling based on recently solved porin crystal structures⁶.

HTS results and the lessons learned

An analysis of the results of 65 high-throughput screens of essential bacterial targets against the AstraZeneca corporate compound collection (TABLE 1) revealed major differences in the overall hit rates, as well as in our definition of leads, as compared to the work at GSK described by Payne *et al.*⁴. The triage and subsequent follow-up of the AstraZeneca campaigns led to three molecule classifications: active, hit and lead. An active was defined as a compound that was above the threshold for noise in a single-concentration screen run in triplicate. A hit was a more generically defined, albeit with project-specific differences. Generally, a hit was defined as a compound with a lack of activity in artefact assays but a reproducible dose response, typically in two separate assays with similar

Table 1 | Summary of HTS results for 65 screens performed at AstraZeneca from 2001–2010

Screen name	Target protein* or activity	Antibacterial class	Species	HTS result
Alr	Alanine racemase (Alr)	Cell wall synthesis inhibitor	<i>Escherichia coli</i>	No hits
Ddl	D-alanine-D-alanine ligase (Ddl)	Cell wall synthesis inhibitor	<i>Streptococcus mutans</i>	Hits with derivatives; no leads
GlmU	UDP-N-acetylglucosamine phosphorylase (GlmU)	Cell wall synthesis inhibitor	<i>Haemophilus influenzae</i>	Leads identified ^{13,14}
GlmU1	Glucosamine-phosphate N-acetyltransferase (GlmU)	Cell wall synthesis inhibitor	<i>E. coli</i>	Leads identified
GlmU2	UDP-N-acetylglucosamine diphosphorylase (GlmU)	Cell wall synthesis inhibitor	<i>Streptococcus pneumoniae</i>	Hits with derivatives; no leads
GlmU3	Glucosamine-1-phosphate N-acetyltransferase (GlmU)	Cell wall synthesis inhibitor	<i>S. pneumoniae</i>	Hits with derivatives; no leads
IspD	4-diphosphocytidyl-2C-methyl-D-erythritol synthase (IspD)	Cell wall synthesis inhibitor	<i>E. coli</i>	No hits
KdsA	3-deoxy-D-manno-octulosonate 8-phosphate synthase (KdsA)	Cell wall synthesis inhibitor	<i>E. coli</i>	No hits
KdsA <i>Helicobacter pylori</i>	3-deoxy-D-manno-octulosonate 8-phosphate synthase (KdsA)	Cell wall synthesis inhibitor	<i>H. pylori</i>	Hits with derivatives; no leads
MurA	UDP-N-acetylglucosamine-enolpyruvyl transferase (MurA)	Cell wall synthesis inhibitor	<i>E. coli</i>	Hits with derivatives; no leads
MurA2	UDP-N-acetylglucosamine 1-carboxyvinyltransferase (MurA2)	Cell wall synthesis inhibitor	<i>S. mutans</i>	Hits with derivatives; no leads
MurB	UDP-N-acetylenolpyruvoylglucosamine reductase (MurB)	Cell wall synthesis inhibitor	<i>Neisseria meningitidis</i>	Hits with derivatives; no leads
MurB2	UDP-N-acetylenolpyruvoylglucosamine reductase (MurB)	Cell wall synthesis inhibitor	<i>E. coli</i>	Hits with derivatives; no leads
MurC	UDP-N-acetylmuramate-L-alanine ligase (MurC)	Cell wall synthesis inhibitor	<i>E. coli</i>	Leads identified ¹⁶
MurC <i>H. pylori</i>	UDP-N-acetylmuramate-L-alanine ligase (MurC)	Cell wall synthesis inhibitor	<i>H. pylori</i>	Hits with derivatives; no leads
MurC2	UDP-N-acetylmuramate-L-alanine ligase (MurC)	Cell wall synthesis inhibitor	<i>Pseudomonas aeruginosa</i>	Hits with derivatives; no leads
MurD	UDP-N-acetylmuramoyl-L-alanine-D-glutamate ligase (MurD)	Cell wall synthesis inhibitor	<i>Enterococcus faecalis</i>	Hits with derivatives; no leads
MurD2	UDP-N-acetylmuramoyl-L-alanine-D-glutamate ligase (MurD)	Cell wall synthesis inhibitor	<i>E. coli</i>	No hits
MurE	UDP-N-acetylmuramoyl-L-alanyl-D-glutamate-2,6-diaminopimelate ligase (MurE)	Cell wall synthesis inhibitor	<i>E. coli</i>	Hits with derivatives; no leads
MurF	UDP-N-acetylmuramoyl-tripeptide-D-alanyl-D-alanine ligase (MurF)	Cell wall synthesis inhibitor	<i>P. aeruginosa</i>	Hits with derivatives; no leads
MurI	Glutamate racemase (MurI)	Cell wall synthesis inhibitor	<i>H. pylori</i>	Hits with derivatives; no leads ¹⁷
MurI3	Glutamate racemase (MurI)	Cell wall synthesis inhibitor	<i>Staphylococcus aureus</i>	Hits with derivatives; no leads
UppS	Undecaprenyl diphosphate synthetase (IspU)	Cell wall synthesis inhibitor	<i>E. coli</i>	Hits with derivatives; no leads
CoaD	Phosphopantetheine adenylyltransferase (CoaD)	Cofactor mimetic	<i>S. mutans</i>	Leads identified ¹⁸
PPAT	Pantetheine-phosphate adenylyltransferase (CoaD)	Cofactor mimetic	<i>S. pneumoniae</i>	Hits with derivatives; no leads
CoaE	Dephospho-CoA kinase (CoaE)	Cofactor mimetic	<i>S. pneumoniae</i>	Leads identified

Table 1 (cont.) | Summary of HTS results for 65 screens performed at AstraZeneca from 2001–2010

Screen name	Target protein* or activity	Antibacterial class	Species	HTS result
NadF	NAD ⁺ kinase (NadK)	Cofactor mimetic	<i>E. coli</i>	Hits with derivatives; no leads
NadK	NAD ⁺ kinase (NadK)	Cofactor mimetic	<i>S. pneumoniae</i>	Hits with derivatives; no leads
RibF	FAD synthetase (RibF)	Cofactor mimetic	<i>S. aureus</i>	Hits with derivatives; no leads
RibF 2nd reaction	FAD synthase, FMN adenylyltransferase (RibF)	Cofactor mimetic	<i>S. aureus</i>	Hits with derivatives; no leads
DnaB	Replicative DNA helicase (DnaB)	DNA synthesis inhibitor	<i>E. coli</i>	Hits with derivatives; no leads
DnaE	DNA polymerase III α (DnaE)	DNA synthesis inhibitor	<i>H. influenzae</i>	Hits with derivatives; no leads
DnaE2	DNA polymerase III α (DnaE)	DNA synthesis inhibitor	<i>S. pneumoniae</i>	Hits with derivatives; no leads
DnaG	DNA primase (DnaG)	DNA synthesis inhibitor	<i>E. coli</i>	Hits with derivatives; no leads
DnaG2	DNA primase (DnaG)	DNA synthesis inhibitor	<i>S. aureus</i>	No hits
Gmk	Guanylate kinase (Gmk)	DNA synthesis inhibitor	<i>E. coli</i>	Hits with derivatives; no leads
LigA	NAD ⁺ dependent DNA ligase (LigA)	DNA synthesis inhibitor	<i>H. influenzae</i>	Leads identified ¹⁹
Ndl	NAD ⁺ dependent DNA ligase (LigA)	DNA synthesis inhibitor	<i>S. pneumoniae</i>	Leads identified
PrsA	Ribose-phosphate diphosphokinase (Prs)	DNA synthesis inhibitor	<i>S. aureus</i>	No hits
PyrH	UMP kinase (PyrH)	DNA synthesis inhibitor	<i>S. aureus</i>	Leads identified ²⁰
PyrH2	UMP kinase (PyrH)	DNA synthesis inhibitor	<i>E. coli</i>	Leads identified
Tmk	dTMP kinase (Tmk)	DNA synthesis inhibitor	<i>S. pneumoniae</i>	Leads identified ²¹
AccAD	Carboxyltransferase activity of acetyl CoA carboxylase (AccA and AccD)	Fatty acid synthesis inhibitor	<i>E. coli</i>	Leads identified
AccC	Biotin carboxylase activity of acetyl CoA carboxylase (AccC)	Fatty acid synthesis inhibitor	<i>E. coli</i>	Leads identified
BirA	Biotin ligase (BirA)	Fatty acid synthesis inhibitor	<i>E. coli</i>	No hits
FabH	β -ketoacyl-(acyl carrier protein) synthase III (FabH)	Fatty acid synthesis inhibitor	<i>E. coli</i>	Leads identified
FabH2	β -ketoacyl-(acyl carrier protein) synthase III (FabH)	Fatty acid synthesis inhibitor	<i>E. coli</i>	Leads identified
LepB	Signal peptidase I (LepB)	Protein secretion inhibitor	<i>E. coli</i>	Hits with derivatives; no leads
Asd	Aspartate semialdehyde dehydrogenase (Asd)	Protein synthesis inhibitor	<i>H. pylori</i>	Hits with derivatives; no leads
MAP	Methionine aminopeptidase (Map)	Protein synthesis inhibitor	<i>E. coli</i>	Hits with derivatives; no leads
Trns1	Ribosome 16S rRNA, paromomycin (aminoglycoside) binding	Protein synthesis inhibitor	<i>E. coli</i>	Hits with derivatives; no leads
TT22	Coupled transcription–translation	Protein synthesis inhibitor	<i>E. coli</i>	Hits with derivatives; no leads
PheRS	Phenylalanine tRNA synthetase (PheS and PheT)	Protein synthesis inhibitor	<i>E. coli</i>	Leads identified ²³
TiIS	tRNA Ile-lysine synthase (TiIS)	Protein synthesis inhibitor	<i>E. coli</i>	Hits with derivatives; no leads
TrmD	tRNA (guanine ³⁷ -N ¹)-methyltransferase (TrmD)	Protein synthesis inhibitor	<i>H. influenzae</i>	Hits with derivatives; no leads
TrmD2	tRNA (guanine ³⁷ -N ¹)-methyltransferase (TrmD)	Protein synthesis inhibitor	<i>H. influenzae</i>	Leads identified ²⁴
Ef-Tu	Nucleotide exchange factor (Ef-Tu–Ef-Ts) interaction (TufA and TufB)	Protein synthesis inhibitor	<i>E. coli</i>	Hits with derivatives; no leads
RNAP	DNA-directed RNA-polymerase (RpoA, RpoB and RpoC)	RNA elongation inhibitor	<i>E. coli</i>	Hits with derivatives; no leads

Table 1 (cont.) | Summary of HTS results for 65 screens performed at AstraZeneca from 2001–2010

Screen name	Target protein* or activity	Antibacterial class	Species	HTS result
SuperC	Supercoiling activity of DNA gyrase (GyrA and GyrB)	Topoisomerase inhibitor	<i>E. coli</i>	Hits with derivatives; no leads
ParE	Topoisomerase IV ATP-hydrolyzing subunit (ParE)	Topoisomerase inhibitor	<i>E. coli</i>	Leads identified
Pae efflux	<i>P. aeruginosa</i> (MexABCDXY) cell survival	Not known (phenotypic screen)	<i>P. aeruginosa</i>	No hits
Waap	<i>E. coli</i> (WaaP) cell survival	Not known (phenotypic screen)	<i>E. coli</i>	Leads identified
Hinf (acrB ⁻)	<i>H. influenzae</i> (AcrB ⁻) cell survival	Not known (phenotypic screen)	<i>H. influenzae</i>	Hits with derivatives; no leads
CWR	Cell wall reporter assay ⁶⁷	Not known (phenotypic screen)	<i>E. coli</i>	Leads identified
AntiB (G-pos)	Cell survival	Not known (phenotypic screen)	<i>S. pneumoniae</i>	Hits with derivatives; no leads

dTMP, deoxy-thymidine monophosphate; HTS, high-throughput screening; UDP, uridine diphosphate, UMP, uridine monophosphate. *Protein abbreviations are indicated in brackets.

conditions but orthogonal detection systems. In evaluating these data, a Hill slope was used as a quality measure, with values between 0.5 and 2.0 typically deemed acceptable for continued evaluation of hits. For targets in which cooperativity was reasonably anticipated amongst inhibitors (for example, in multimeric enzymes such as phosphopantetheine adenyltransferase (CoaD))⁷ a higher Hill slope of 3.0 was allowed. In retrospect, however, none of the lead series that was progressed maintained a Hill slope above 2.0. Hits were also evaluated for acceptable chemical properties and, typically, activity across a broad spectrum of bacterial isozymes (for broad-spectrum projects).

A lead was defined as an example member of a hit series for which we had an understanding of how to optimize the drug-like properties and an evidence-based hypothesis of how to obtain antibacterial whole cell activity, and was a compound that demonstrated a progressable structure–activity relationship (SAR), a lack of mammalian cytotoxicity and a target-specific mechanism of inhibition. The last criterion was viewed as essential, but it could be difficult to interpret for earlier hit series for which, at the time, weak (or no) antimicrobial activity was measurable, and thus, straightforward selection of resistant mutants was not possible. As such, the mechanism of inhibition was evaluated through a holistic approach that combined both enzyme kinetics and binding studies to establish confidence in inhibitor modality⁸ and, typically, selectivity against the human homologue, if present. These results were further evaluated in conjunction with cellular studies, in which inhibition

of the anticipated target functions in intact cells was evaluated. A discussion of possible approaches to this problem has recently been published⁹, but it is beyond the scope of this Opinion article. However, as an example, radioactive macromolecule incorporation studies may provide early indications of appropriate cellular target engagement, and in the case of Gram-negative organisms these studies can be performed in an efflux-attenuated strain, as the dose response may occur below the minimum inhibitory concentration (MIC)¹⁰. Alternatively, projects may track a specific metabolite or macromolecule, or, for compounds with antibacterial activity, projects can track potency loss in a strain overexpressing the target¹¹.

The criteria we used for hits and leads seem to be in line with those reported by Payne *et al.*⁴, with two possible differences that may be difficult to assess. First, definitions of chemical tractability are not easy to compare between the two groups, an issue that has been previously discussed regarding medicinal chemistry bias¹². Second, we identified active compounds for more targets than did previous reports. Although we cannot fully understand this difference without a direct case-by-case comparison, our definition of a hit may have been more permissive than the low micromolar activity required in previous efforts.

Overall, the process of triaging high-throughput screens was implemented to rigorously interrogate a high volume of projects, anticipating high attrition rates. As such, the incentive for the hit-to-lead teams at the time was to quickly identify the most promising opportunities and to avoid diverting resources to risky or

difficult-to-optimize series. One consequence of this strategy was that the triage during these early stages commonly employed filters such as undesirable chemical features, mammalian cytotoxicity and predicted off-target effects, such as inhibition of the human ether-à-go-go-related gene potassium channel 1 (ERG)¹³. These practices were adopted to cope with the sheer volume of hit lists, and they arguably discouraged medicinal chemistry teams from developing an understanding of how tightly these detrimental features were coupled with desirable SAR, potentially resulting in the premature elimination of viable chemical compounds. Therefore, the hit-to-lead conversion rates presented here probably represent conservative estimates of the suitability of the library for screening against antibacterial targets.

Of the 65 campaigns, 57 identified hits (TABLE 1). Notable exceptions included the IspD, MurD2 and DnaG2 screens, which assayed for the activity of 4-diphosphocytidyl-2-methyl-D-erythritol synthase (IspD), uridine diphosphate (UDP)-*N*-acetylmuramoyl-L-alanine-D-glutamate ligase (MurD) and DNA primase (DnaG), respectively, and did not identify biochemically active molecules. For example, a triage of the most promising molecules with activity against IspD resulted in no compounds that passed the biochemical criteria. In this case, 200 compounds were tested in dose–response assays, but all of the compounds that had a measurable IC₅₀ also demonstrated behaviour consistent with aggregation (such as a large IC₅₀ ratio when run in a second assay at a higher enzyme concentration)¹⁴.

Table 2 | Summary of hits and the confirmed chemical series that were pursued as a result of these screening efforts

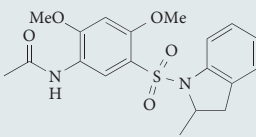
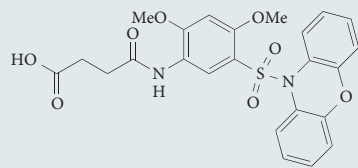
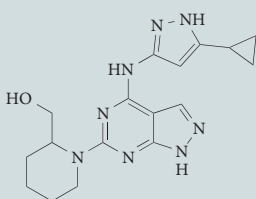
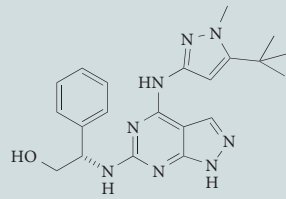
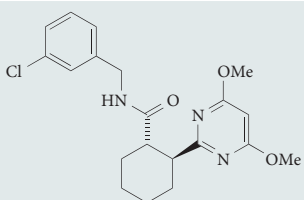
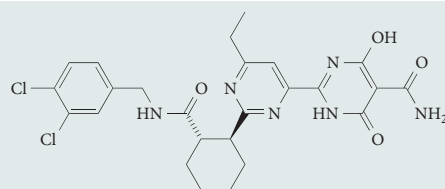
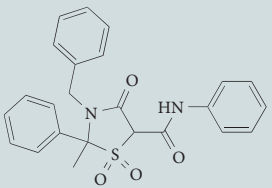
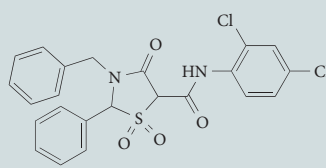
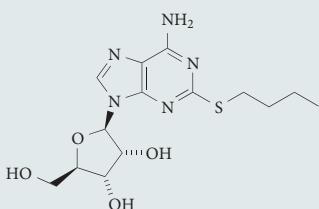
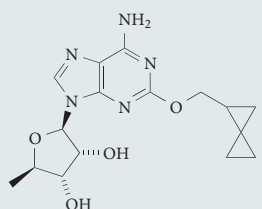
Target	Number of HTS actives	Number of hits	Example hit structure	Example lead structure
GlmU	10,012	2	 <p><i>Haemophilus influenzae</i> (GlmU) $IC_{50} = 7.8 \mu M$ <i>H. influenzae</i> (AcrB) MIC >64 $\mu g mL^{-1}$ cLogD* = 1.79</p>	 <p><i>H. influenzae</i> (GlmU) $IC_{50} = 0.023 \mu M$ <i>H. influenzae</i> (AcrB) MIC = 32 $\mu g mL^{-1}$ cLogD = -0.40</p>
MurC	799	90	 <p><i>Pseudomonas aeruginosa</i> $IC_{50} = 1.0 \mu M$ <i>P. aeruginosa</i> MIC >64 $\mu g mL^{-1}$ cLogD = 2.68</p>	 <p><i>P. aeruginosa</i> $IC_{50} = 0.001 \mu M$ <i>P. aeruginosa</i> (MexABCDXY) MIC = 1.5 $\mu g mL^{-1}$ <i>P. aeruginosa</i> MIC >64 $\mu g mL^{-1}$ cLogD = 3.35</p>
CoaD	3,814	114	 <p><i>Staphylococcus aureus</i> $IC_{50} = 7.3 \mu M$ <i>Streptococcus pneumoniae</i> $IC_{50} = 0.20 \mu M$ cLogD = 2.97</p>	 <p><i>S. aureus</i> $IC_{50} = 0.00087 \mu M$ <i>S. pneumoniae</i> $IC_{50} = 0.000065 \mu M$ <i>Staphylococcus aureus</i> MIC = 0.12 $\mu g mL^{-1}$ <i>S. pneumoniae</i> MIC = 0.03 $\mu g mL^{-1}$ In vivo active at 100 mg kg^{-1} <i>S. pneumoniae</i> cLogD = 2.06</p>
CoaE	1,398	10	 <p><i>Escherichia coli</i> (CoaE) $IC_{50} = 13 \mu M$ <i>H. influenzae</i> (CoaE) $IC_{50} = 30 \mu M$ cLogD = 2.26</p>	 <p><i>E. coli</i> (CoaE) $IC_{50} = 1.7 \mu M$ <i>H. influenzae</i> (CoaE) $IC_{50} = 7.8 \mu M$ cLogD = 2.07</p>
LigA	5,742	31	 <p><i>H. influenzae</i> $IC_{50} = 0.50 \mu M$ <i>S. aureus</i> $IC_{50} = 0.081 \mu M$ cLogD = 1.40</p>	 <p><i>H. influenzae</i> $IC_{50} = 0.082 \mu M$ <i>H. influenzae</i> MIC = 8 $\mu g mL^{-1}$ <i>S. aureus</i> $IC_{50} = 0.06 \mu M$ <i>S. aureus</i> MIC = 2 $\mu g mL^{-1}$ cLogD = 1.78</p>

Table 2 (cont.) | Summary of hits and the confirmed chemical series that were pursued as a result of these screening efforts

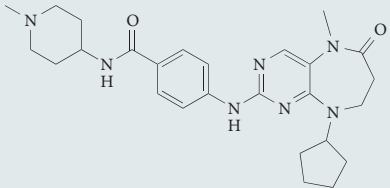
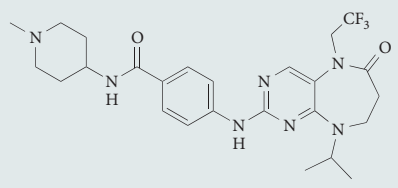
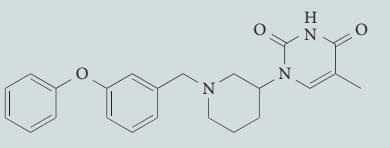
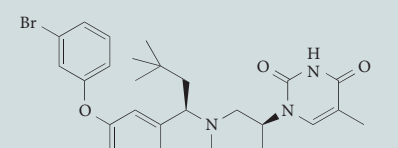
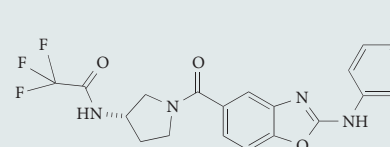
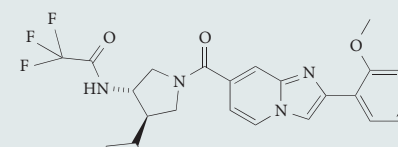
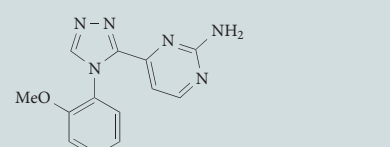
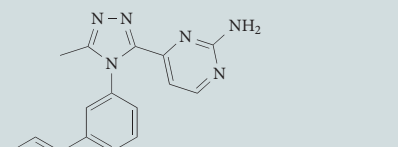
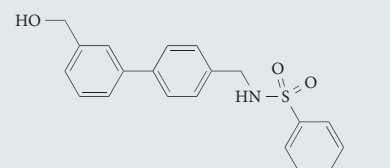
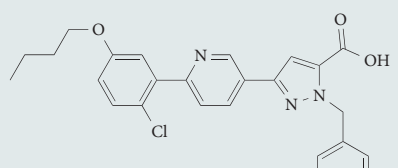
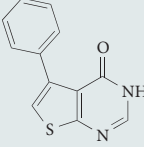
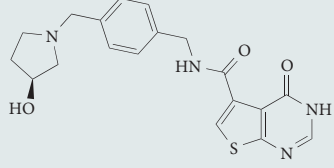
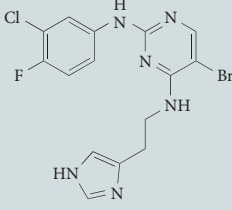
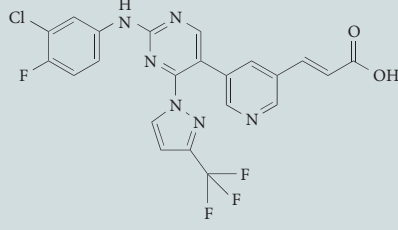
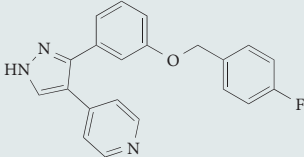
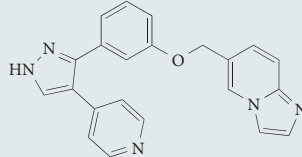
Target	Number of HTS actives	Number of hits	Example hit structure	Example lead structure
PyrH	5,312	59	 <p><i>E. coli</i> IC₅₀ = 10 μM cLogD = 2.05</p>	 <p><i>E. coli</i> IC₅₀ = 0.7 μM <i>E. coli</i> (TolC-) MIC > 200 μM <i>E. coli</i> MIC > 200 μM cLogD = 2.02</p>
Tmk	1,273	16	 <p><i>S. pneumoniae</i> IC₅₀ = 3.4 μM cLogD = 2.97</p>	 <p><i>S. pneumoniae</i> IC₅₀ = 0.0002 μM <i>S. pneumoniae</i> MIC = 0.01–0.02 μg mL⁻¹ cLogD = 1.16</p>
AccA and AccD	3,341	39	 <p><i>S. aureus</i> IC₅₀ = 7.24 μM <i>S. aureus</i> MIC > 200 μM cLogD = 2.63</p>	 <p><i>S. aureus</i> IC₅₀ = 0.035 μM <i>S. aureus</i> MIC = 50 μM cLogD = 3.77</p>
AccC	6,105	67	 <p><i>E. coli</i> IC₅₀ = 9.0 μM <i>E. coli</i> (TolC-) MIC > 200 μM cLogD = 0.34</p>	 <p><i>E. coli</i> IC₅₀ = 0.10 μM <i>E. coli</i> (TolC-) MIC = 12.5 μM cLogD = 2.00</p>
FabH	7,629	112	 <p><i>E. coli</i> IC₅₀ = 15 μM <i>S. aureus</i> IC₅₀ > 200 μM cLogD = 3.05</p>	 <p><i>S. aureus</i> IC₅₀ = 0.018 μM <i>S. aureus</i> MIC = 25 μM cLogD = 2.62</p>

Table 2 (cont.) | Summary of hits and the confirmed chemical series that were pursued as a result of these screening efforts

Target	Number of HTS actives	Number of hits	Example hit structure	Example lead structure
TrmD	1,281 (FBLG)	18	 <p><i>S. aureus</i> IC₅₀ = 7.24 μM <i>S. aureus</i> MIC >200 μM cLogD = 2.13</p>	 <p><i>S. aureus</i> IC₅₀ = 0.035 μM <i>S. aureus</i> MIC = 50 μM cLogD = 0.42</p>
ParE	2,127	111	 <p><i>E. coli</i> IC₅₀ = 5 μM <i>S. pneumoniae</i> IC₅₀ = 17 μM cLogD = 3.50</p>	 <p><i>E. coli</i> IC₅₀ = 0.07 μM <i>S. pneumoniae</i> IC₅₀ = 0.001 μM <i>S. pneumoniae</i> MIC = 0.006 μM cLogD = 2.30</p>
CWR assay ⁶⁷	5,719	106	 <p><i>E. coli</i> (TolC) IC₅₀ < 0.06 μg mL⁻¹ <i>E. coli</i> = 8 μg mL⁻¹ cLogD = 4.37</p>	 <p><i>E. coli</i> (TolC) IC₅₀ < 0.06 μg mL⁻¹ <i>E. coli</i> = 2 μg mL⁻¹ cLogD = 3.57</p>

AccA, acetyl-CoA carboxyltransferase α -subunit; AccC, biotin carboxylase; AccD, acetyl-CoA carboxyltransferase β -subunit; CoaD, phosphopantetheine adenyltransferase; CoaE, dephospho-CoA kinase; CWR, cell wall reporter; FabH, β -ketoacyl-(acyl carrier protein) synthase III; FBLG, fragment-based lead generation; GlmU, uridine diphosphate (UDP)-*N*-acetylglucosamine phosphorylase; HTS, high-throughput screening; IC₅₀, inhibitor concentration at 50% effect; LigA, NAD⁺ dependent DNA ligase; MIC, minimum inhibitory concentration; MurC, UDP-*N*-acetylmuramate-L-alanine ligase; ParE, topoisomerase IV ATP-hydrolyzing subunit; PyrH, uridine monophosphate kinase; Tmk, deoxy-thymidine monophosphate kinase; TrmD, tRNA (guanine³⁷-N¹)-methyltransferase. *cLogD is the 'computed' LogD, using AstraZeneca's proprietary predictive model, AZlogD_{z4}.

Of the 57 programmes for which hits were identified, 19 found leads after the hits were further investigated and refined by our chemistry team. These analyses to identify leads were based on molecules with a plausible SAR for the biochemical target, selectivity over mammalian cell cytotoxicity and a good range of biochemical activity that was dependent on the target bacteria: typically for Gram-positive targets, our teams were seeking activity against *S. aureus* and *S. pneumoniae*; for Gram-negative targets, activity against *P. aeruginosa* and *A. baumannii* were desired to progress efforts.

Reasons for attrition. The large degree of attrition seen in the identification of antibacterial compounds was probably driven by several causes. Some of these are common to many HTS projects outside of antibacterial

drug discovery, such as a lack of a confirmed dose response or interference with assay-detection methodology as confirmed in orthogonal assays. However, some of the attrition is unique to the identification of novel antibacterials. At the time of many of these screens, the commercially viable (and therefore accepted) therapeutic profile was broad-spectrum activity against both Gram-positive and Gram-negative organisms. This paradigm meant that the HTS strategy and hit triage required biochemical activity across a panel of isozymes from several relevant Gram-positive and Gram-negative organisms for a molecule to progress. This paradigm has since shifted, and target-specific pathogen approaches may now have a regulatory and commercial path forward³, which was not the perception during the era of HTS and biochemical screening of antibacterial targets.

Another factor that led to very high attrition was the attempt to incorporate many drug-like properties upfront to generate chemical matter suitable for both intravenous and oral formulation. In addition, a substantial proportion of hits were discarded on the basis of presumed chemical undesirability and/or toxicity, usually based on particular chemists' prior experience with similar or related compounds¹². Finally, a stringent filter was implemented to ensure that the growth of human cell lines (mainly A549 lung carcinoma cells) was not inhibited in order to mitigate potential for toxicity early in the screening funnel. This filter was intended to remove compounds that were intrinsically toxic to both human and bacterial cells through a shared mechanism; however, it is also likely that the filter removed antibacterial compounds that coincidentally

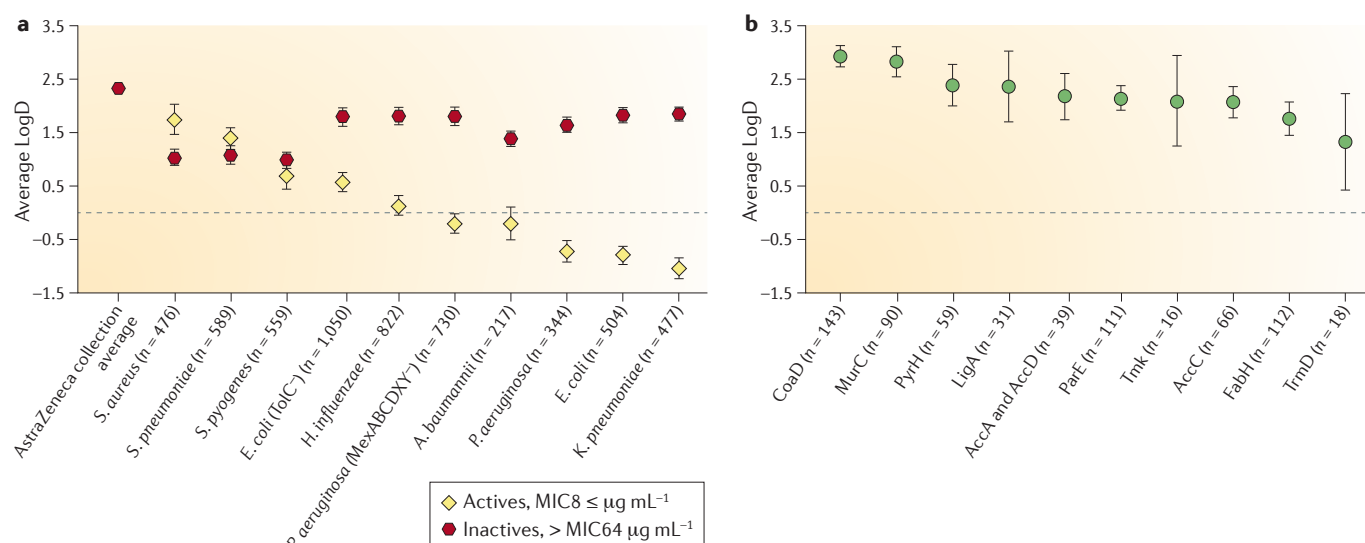


Figure 1 | Mean LogD values for internal AstraZeneca antibacterial project compounds and for exemplar hits from other disease areas.

The mean LogD values were calculated at pH 7.4 using AstraZeneca internal software that was parameterized on a continual basis using new data. Error bars indicate the 99% confidence interval for the mean of calculated LogD values for each category on the x axis. **a** | The mean LogD values for active compounds targeting 10 key pathogens are indicated by yellow diamonds, and the number of active compounds (n) with a minimum inhibitory concentration (MIC) $\leq 8 \mu\text{g mL}^{-1}$ is indicated in parentheses. The mean LogD values of inactive compounds (MIC $> 64 \mu\text{g mL}^{-1}$) are indicated by red hexagons. The mean of a random sample of 45,000 compounds from the AstraZeneca screening collection is shown for reference. **b** | The mean LogD values for hits from ten representative high-throughput screens are

indicated by green circles, and the number of hits (n) included in the analysis is indicated in parentheses. *A. baumannii*, *Acinetobacter baumannii*; AccA, acetyl-CoA carboxyltransferase α -subunit; AccC, biotin carboxylase; AccD, acetyl-CoA carboxyltransferase β -subunit; CoaD, phosphopantetheine adenyltransferase; *E. coli*, *Escherichia coli*; FabH, β -ketoacyl-(acyl carrier protein) synthase III; *H. influenzae*, *Haemophilus influenzae*; *K. pneumoniae*, *Klebsiella pneumoniae*; LigA, DNA ligase; MurC, uridine diphosphate (UDP)-N-acetylmuramate-L-alanintransferase; *P. aeruginosa*, *Pseudomonas aeruginosa*; ParE, topoisomerase IV; PyrH, uridine monophosphate (UMP) kinase; *S. aureus*, *Staphylococcus aureus*; *S. pneumoniae*, *Streptococcus pneumoniae*; *S. pyogenes*, *Streptococcus pyogenes*; Tmk, deoxy-thymidine monophosphate (dTMP) kinase; TrmD, tRNA (guanine³⁷-N¹)-methyltransferase.

exhibited mammalian cell toxicity through distinct mechanisms that might have been circumvented during lead identification and optimization.

Hits to leads. From these screening efforts, 19 programmes identified viable hits that were further advanced with exploratory chemistry efforts (13 examples are shown in TABLE 2) — an important distinction from the efforts previously reported by GSK⁴, wherein no hits were identified for many of these targets. Although finding hits with biochemical activity was not unusual for these screens, finding hits with whole-cell wild-type antibacterial activity in relevant pathogens without equipotent mammalian cell cytotoxicity was a rare event — only the cell wall reporter (CWR) screen led to such a compound (TABLE 2). However, similar to the efforts of GSK, in most cases leads that exhibited antimicrobial activity had to be derived from early optimization efforts and so, in these situations, the decision to optimize the molecule through iterative chemical modifications was made before cellular antibacterial activity (as measured by MIC¹⁵) was obtained.

Thus, the main objective of these early optimization campaigns was to probe the SAR of the series in hand and determine whether cellular activity could be achieved. Of the 19 programmes with progressable chemical matter, several led to potent antibacterial activity in Gram-positive bacteria with efficacy in animal models (including those targeting CoaD⁷, topoisomerase IV (ParE)¹⁶ and deoxy-thymidine monophosphate (dTMP) kinase (Tmk)¹⁷); however, none of the programmes led to novel and potent Gram-negative antibacterial development candidates. Some of the reasons for this are explained below.

Physicochemical property trends. A physicochemical property analysis allowed us to conclude that many antibacterial targets exhibited a preference for compounds with substantially higher lipophilicity than was optimal for maintaining bacterial permeability, particularly when compounds targeting Gram-negative pathogens were analysed. In a recent publication¹⁸, we presented a detailed analysis of HTS output and compared the physical properties of ~3,200 compounds — synthesized for internal

antibacterial programmes over the past 3 years — that were run against a panel of important pathogens (both wild-type and permeabilized mutants). Compounds that had antibacterial activity against any of the pathogens at a concentration of $\leq 8 \mu\text{g mL}^{-1}$ were included in the analysis, and their activity was compared to the physicochemical properties of HTS actives generated from other AstraZeneca screening campaigns over the past 5 years (FIG. 1). Notably, the lowest LogD values were observed among those bacterial species with the fewest treatment options (FIG. 1). Many HTS actives have much higher lipophilicities than typical actives against important pathogens. There are exceptions, including hydrophobic compounds such as inhibitors of the deacetylase LxpC, which do show good cellular activity. However, these exceptions frequently come with a range of issues associated with high lipophilicity, including high levels of plasma protein binding, cytotoxicity, efflux and off-target promiscuity^{19–21}. Furthermore, for some targets the average lipophilicity of biochemical actives and hits is even higher than the collection average. This raises the possibility that such screens may select

for hydrophobic binding sites that favour intrinsic binding energetics, which further bias molecules towards having LogD values above what is normally seen for marketed antibacterial agents. Although many progressable hits were identified for most of the AstraZeneca screening targets, the progression of these projects into lead optimization proved extremely difficult, as hits were typically ~3–4 log units more hydrophobic than the average hydrophobicity of a typical antibacterial agent (FIG. 2).

In response to the lack of molecules with whole-cell activity for use as starting molecules in our programmes, conventional wisdom amongst medicinal chemists often supported design strategies that drive biochemical potency to nanomolar levels to achieve meaningful activity (typically single-digit micromolar) against intact bacteria, often with this observation extending to include even hypersensitive mutant strains. Although this may have been an accepted strategy in the field during the HTS era of antibacterial drug discovery, several examples presented here demonstrate the limitations of this approach. For example, for inhibitors of UDP-*N*-acetylmuramate-*L*-alanine ligase (MurC) or CoaD, nanomolar activity was achieved without marked antibacterial activity. Conversely, the strategy of only driving potency against the target has not received universal support. Indeed, privileged scaffolds or targets exist for which good antibacterial activity can be achieved without large differences between the target-binding and whole-cell activity potencies. One such example is the group of benzoxaborole-derived inhibitors that target leucyl-tRNA synthetase²². These inhibitors typically had only micromolar biochemical activity but nonetheless exhibited impressive antibacterial potency. Clearly, a detailed understanding of the cellular context of the target, and whether or not its corresponding biochemical assay adequately represents physiological conditions, is key for successful execution of this strategy.

Although it is simple to suggest that teams should focus on designing compounds with a low LogD as well as simultaneously increasing the biochemical potency, in our experience, lipophilicity typically increases with potency. This tendency is highly dependent on the nature of the target binding site; however, lipophilic compounds are difficult to avoid for targets with large hydrophobic active sites. For example, in identifying compounds that inhibit MurC (FIG. 2), chemists that were designing and synthesizing compounds over the course

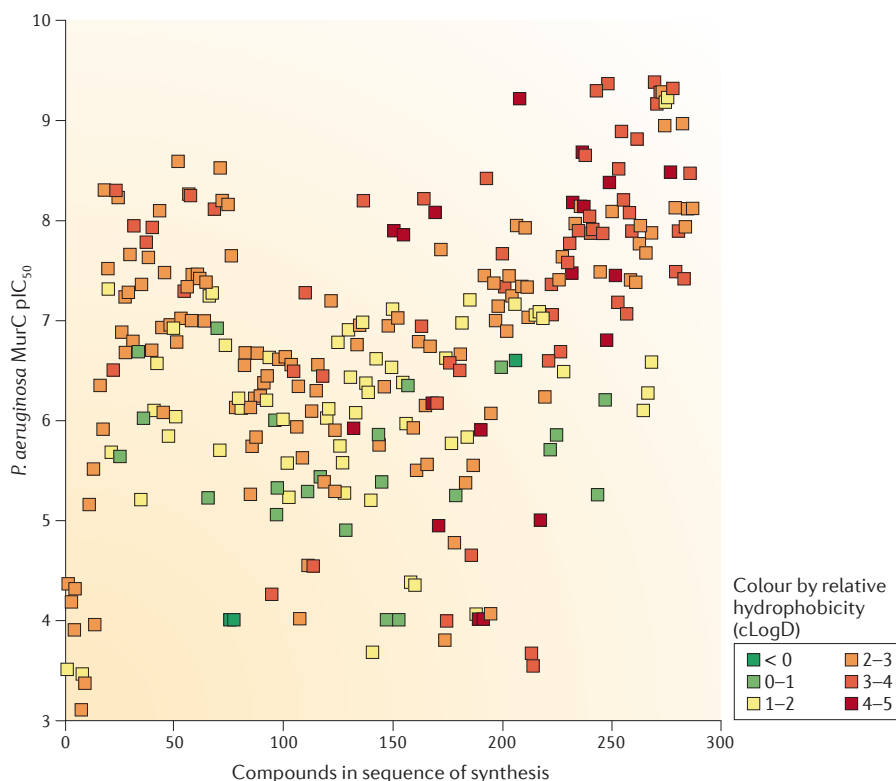


Figure 2 | The relationship over time between the biochemical potency against *Pseudomonas aeruginosa* MurC and the cLogD of newly synthesized programme compounds. As chemists were designing and synthesizing compounds over the course of the project (shown as sequential compound registrations on the x axis) the most potent examples trended towards having a high hydrophobicity (dark red squares). Efforts to reduce the hydrophobicity were generally met with reduced biochemical potency (green squares). The molecules are grouped by hydrophobicity, as measured by ‘computed’ LogD (cLogD) values, calculated using AstraZeneca’s proprietary predictive model, AZlogD_{1,4}, as indicated in the key.

of the project encountered a very common problem: the most potent compounds that the teams generated tended to be very hydrophobic (FIG. 2). Efforts to reduce lipophilicity are generally met with reduced biochemical potency (FIG. 2), which further exacerbates the separation between their activity and the MICs in important pathogens²³. Teams may eventually give up trying to find hydrophilic compounds and focus on the hydrophobic compounds, hoping to identify compounds potent enough to negate the loss of activity due to outer membrane permeability barriers. We have found that this approach generally does not work.

The AstraZeneca team also screened several diverse chemical libraries with a range of physical properties and characteristics outside of the typical screening collection with the hopes of overcoming some of the abovementioned issues. Phenotypic screens were also pursued in an attempt to identify compounds with acceptable MICs from the start of the programme. Neither

target-based nor phenotypic screening approaches against these diverse libraries yielded any substantial differences in hit frequency when compared to the standard AstraZeneca proprietary screening sets used in the 65 high-throughput screens highlighted above. In many of these efforts hydrophobicity remained an issue, such that the most interesting molecules identified still exhibited a LogD >3, even when present in smaller numbers among the original screening sets¹⁸.

It should also be noted that having chemical series in the appropriate physical property space does not automatically increase the probability of finding whole-cell active compounds. For example, compounds that inhibit β -ketoacyl-(acyl carrier protein) synthase III (FabH) had favourable physical properties (FIG. 1), but only a few examples exhibited very weak activity in Gram-positive strains and no activity in Gram-negative strains. There are several obvious reasons for this observation, including a lack of target

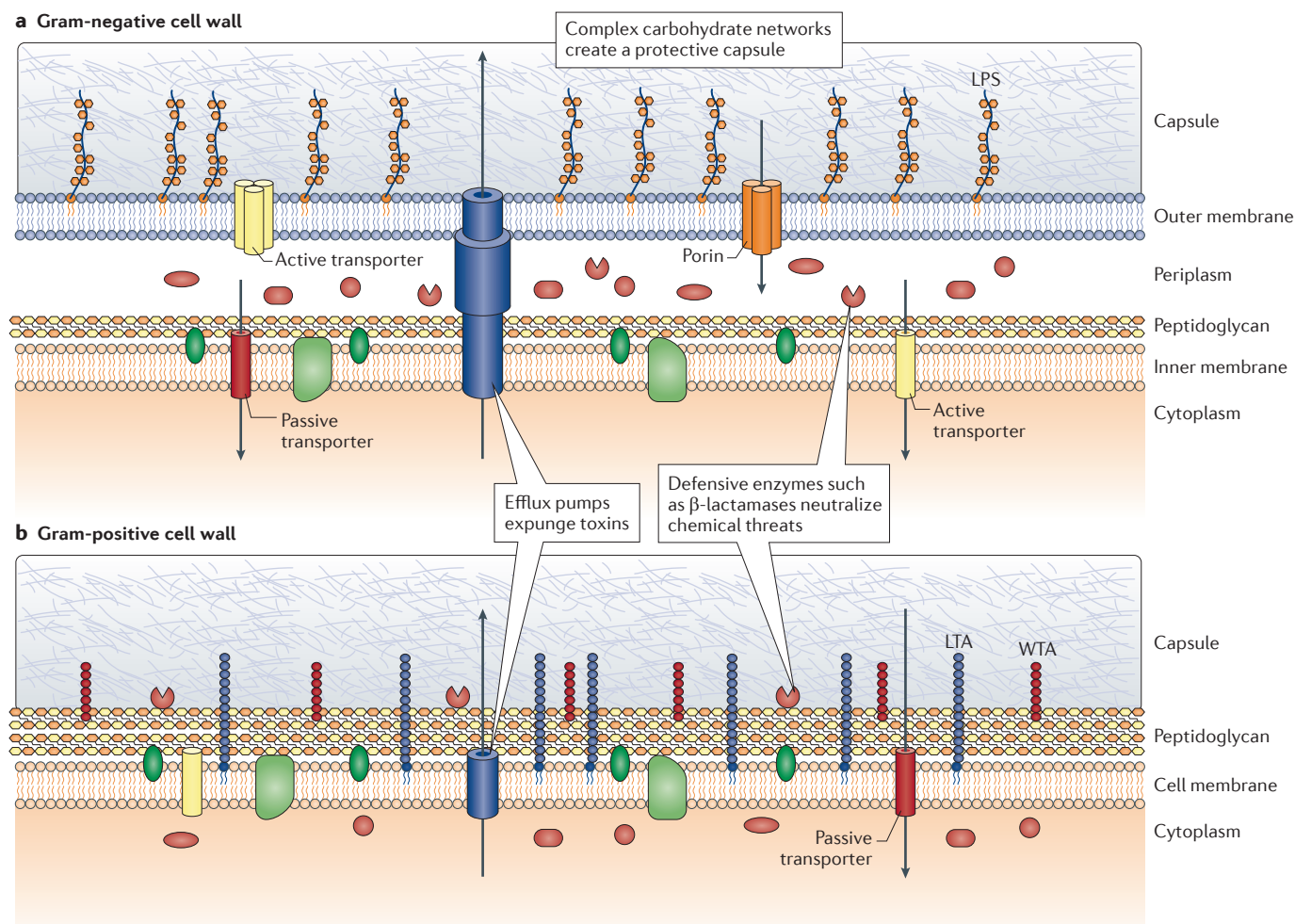


Figure 3 | Gram-negative and Gram-positive cell walls. Gram-negative bacteria rely on both an inner and an outer membrane surrounding a thin peptidoglycan matrix and a periplasmic space (part **a**), whereas Gram-positive bacteria generally use a thicker peptidoglycan layer to protect a single cytoplasmic membrane (part **b**)²⁷. Transport of antibiotics and other extracellular compounds across bacterial membranes occurs both actively and passively, depending on the nature of the

transporter. There are numerous components associated with both types of cell walls that limit the ability of antibiotics to penetrate these structures, such as efflux pumps that expunge toxins, defensive enzymes, such as β -lactamases, and complex carbohydrate networks that create a protective capsule coating. Integral and peripheral membrane proteins are shown in light and dark green, respectively. LPS, lipopolysaccharide; LTA, lipoteichoic acid; WTA, wall teichoic acid.

affinity and engagement, translocation of the drug across the bacterial membrane and whether the target protein is essential.

Screening of natural products was once a rich source of antibacterial leads and drugs for the pharmaceutical industry. Although there continue to be recent examples of important new discoveries (for example, teixobactin, which was discovered from previously ‘unculturable’ microbes²⁴) many large pharmaceutical companies have divested their natural product platforms in favour of more-general screening collections that can target multiple therapy areas. Numerous pharmaceutical companies, including ours, have wondered whether a return to natural product screening may address some of the issues highlighted above, as natural products

have chemical properties that are diverse from typical corporate screening collections; for example, many natural products are highly polar, zwitterionic or bind their targets covalently²⁵. In addition to their chemical diversity, these natural products use specific bacterial-membrane penetration mechanisms (which are often unknown) that are even more important for antibacterial discovery. It is our belief that reinvestment solely in general natural product screening to find new antibacterial natural products may not be as valuable as a strategy that also aims to understand the detailed mechanisms by which many of these large structures penetrate not only the outer membrane but also, in some cases, the cytoplasmic membrane of Gram-negative pathogens.

Getting drugs into bugs

Our experience indicates that there are a number of essential bacterial targets that could be more successfully pursued if research teams had a better understanding of how to design molecules that efficiently permeate bacteria, especially Gram-negative species. Here we describe innovative approaches to address this knowledge gap.

A defining feature of the bacterial cell wall is peptidoglycan, a cross-linked polymer that provides mechanical strength and structure, the thickness and shape of which is species dependent²⁶ (FIG. 3). Gram-positive bacteria generally use a thick peptidoglycan layer to protect a single cytoplasmic membrane, whereas Gram-negative bacteria rely

on both an inner and an outer membrane surrounding a thinner peptidoglycan matrix and a periplasmic space²⁷. There are numerous components associated with both types of cell walls that limit the ability of antibiotics to penetrate these structures, including efflux pumps that expunge toxins, defensive enzymes (such as β -lactamases) and complex carbohydrate networks that create a protective capsule coating²⁷. In particular, the Gram-negative outer membrane can be highly impermeable in certain non-fermenting bacterial species, such as *Pseudomonas aeruginosa* and *Acinetobacter baumannii*, providing them with an extremely effective barrier to the vast majority of molecules, except those required for growth and metabolism²⁸. In these organisms, nutrients are permitted access through the outer membrane by a handful of active transport systems and by passive β -barrel transport proteins, some of which can exhibit a surprising degree of selectivity. For example, *P. aeruginosa* encodes genes for more than 30 porins²⁹ and has a number of subfamilies specific for amino acids, sugars and even phosphate. Among these, mutations in *occD1* (also known as *oprD*; encoding OccD1) confer resistance to carbapenems, implicating porins in the uptake of these antibiotics. Although the contribution of efflux systems and other defence mechanisms cannot be overlooked, a detailed understanding of the key interactions leading to compound recognition by, and passage via, porins such as OccD1 may help to enable the design of molecules with improved permeation across this barrier in these important pathogens. Ultimately, this understanding may lead to more effective antibiotics, especially those

Box 1 | Tn-seq in antibacterial research

Next-generation transposon junction sequencing (Tn-seq) combines the power of transposon mutagenesis with next-generation sequencing³⁷. The approach relies on the availability of a saturated library of transposon mutants that has been generated in a bacterial strain of interest. Total genomic DNA (gDNA) is isolated from the transposon library after it has been grown under the desired experimental condition, such as passage through an infection model or treatment with an antibiotic. Once harvested and purified from surviving bacteria, total gDNA is sheared and PCR-amplified using oligonucleotides that contain both transposon-specific sequences and 'barcodes' that allow for high-throughput sequencing of transposon junctions. After massive parallel sequencing is performed, the barcodes are used to map each transposon back to the genome. The contribution of each gene to the overall fitness of the bacteria during the experiment can therefore be calculated by comparing the frequency of occurrence of each mutant before and after treatment, as the change in frequency reflects the effect of the mutation on bacterial survival under those conditions. In addition to revealing roles for individual genes, this method allows for accurate and quantitative determination of genetic interactions on a genome-wide scale. Tn-seq also has an advantage over traditional microbial genetic screens (which often rely on relatively stringent, positive selection) and target identification and/or validation during the course of infection, as it does not depend on a pre-existing, defined set of insertionally inactivated strains (although confirmation of any observed patterns still requires the generation and characterization of individual mutants). However, as with traditional approaches, the results from this method are limited to non-essential genes. Although most applications of Tn-seq to date have focused on the characterization of fitness and/or virulence determinants in a wide variety of bacterial pathogens (such as *Staphylococcus aureus*⁵², *Escherichia coli*⁵³, *Yersinia pestis*⁵⁴, *Acinetobacter baumannii*⁵⁵ and *Pseudomonas aeruginosa*^{56,57}) it has also been used for target identification⁵⁸ and to identify mechanisms of antibiotic activity (see the Discuva website) and resistance⁵⁹. Other systems-level platforms that are complementary to Tn-seq, such as RNAseq^{60–62}, microbial proteomics^{63,64} and metabolomics^{65,66}, also have great potential to become useful in antibiotics research; however, a detailed description of these emerging technologies is beyond the scope of this Opinion article.

that target proteins in the periplasmic space (inhibitors of Gram-negative cytoplasmic targets obviously face the additional challenge of traversing both the periplasm and the inner membrane). The following detailed examination of OccD1 helps to illustrate this concept.

The X-ray crystal structure of OccD1 revealed a channel formed by an 18-strand β -barrel and a lumen characterized by a basic ladder of arginine residues that is thought to participate in substrate

recognition and translocation³⁰. The structures of a large number of porins from the outer-membrane carboxylate channel (Occ) family have also been solved⁶, showing overall conservation of the folding and tertiary structure within the family and highlighting variations in a putative recognition pocket. However, among the members of these porin families there are also amino acid variations in the otherwise conserved basic ladder, suggesting that substrate recognition might not be localized in these systems but rather that several recognition elements might work together to achieve high substrate specificity without the tight binding that is generally observed for ligand–receptor interactions in structure-based drug design.

Molecular simulations have been used to model the overall kinetics of translocation that result from the multiple transient interactions between a porin and its substrate^{31–33}. A key challenge to *in silico* approaches for studying kinetic processes is the need for relatively long and atomically detailed simulations to adequately sample key interactions that contribute to the free-energy profile for translocation. These simulations require vast amounts of computer time, specialized hardware³⁴ or clever but potentially error-prone sampling schemes. Metadynamics is one such sampling technique that applies small repulsive

Glossary

cLogD

The 'computed' LogD, using a predictive model. The values in this paper were calculated using AstraZeneca's proprietary model, AZLogD_{7,4}.

Hill slope

A measure of binding or linkage cooperativity that can reflect a deviation from simple 1:1 stoichiometry (for which the Hill slope is equal to 1). The term is named in honour of A. V. Hill, the recipient of the 1922 Nobel Prize in Physiology or Medicine.

IC₅₀

Inhibitor concentration at 50% effect. This is a generalized measure of inhibitory potency for a dose response, and dependent upon the conditions of the specific assay. Ideally, the relationship between this result and the intrinsic binding inhibition constant (K_i) may be understood from mechanism of inhibition studies.

LogD

The distribution coefficient, measured as the relative partitioning of all ionizable forms of a small molecule between a hydrophobic (octanol) and aqueous phase buffered to a particular pH, usually 7.4. This term describes the relative hydrophobicity of a chemical compound and is different to the related partition coefficient, logP, which describes the partitioning of only the neutral (non-ionized) form of the compound between phases.

Minimum inhibitory concentration

This measurement reflects the lowest concentration of compound that visibly inhibits the growth of an organism after overnight incubation.

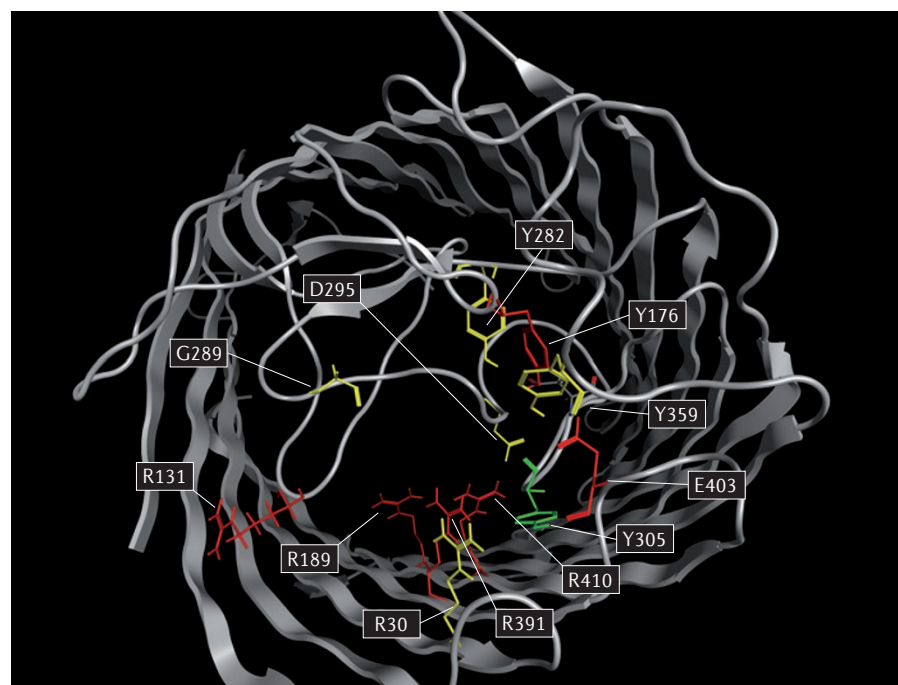


Figure 4 | Effect of porin point mutations on antibiotic transport. Crystal structure of the porin OccD1 (Protein Data Bank identifier: 3SY7)^{6,30}, illustrating the effect of point mutations in the porin on translocation of meropenem³⁶. The locations of the point mutations are indicated by white boxes, and the effects of the point mutations are colour coded: red indicates a reduction in permeability, yellow indicates no effect and green indicates an increase in permeability.

forces to each state visited by a system in order to overcome barriers on the potential energy surface, encouraging the surface to sample new configurations³⁵. Combined with clusters of (inexpensive) graphical processing units, these techniques enable the mapping of the free energy profile for translocation through the porin with a few hours of computer time. We have recently used this technology to construct an *in silico* platform for the high-throughput evaluation of compounds in the OccD family of porins (OccD1 and OccD3), and we used this platform to gain insights into the differences in permeability between imipenem, which mimics the native OccD1 substrate arginine, and meropenem³⁶.

A basic understanding of the complex interplay of mechanisms driving compound uptake across bacterial membranes is an absolute prerequisite for the rational design of compounds with higher affinity and/or rates of transport. We can now complement the powerful computational methods described above with a variety of biological tools that characterize bacterial physiology on a global scale, such as next-generation transposon junction sequencing (Tn-seq)³⁷ (BOX 1). Recently, we used this approach to assess the contribution of all potential outer

membrane transporters to carbapenem uptake by *P. aeruginosa* by identifying transposon-induced mutants in genes encoding outer membrane transporters that were substantially enriched after drug treatment. Although this study focused on outer membrane transporters, it is important to note that, due to its global nature, Tn-seq generates data related to all mechanisms of resistance, not just the reduction of compound uptake. We found that carbapenems are transported not only by OccD1 (as has been well-established in the literature) but also by a closely related channel, OccD3 (also known as OpdP)³⁶. Although identification of this alternative uptake mechanism is logical, considering the high homology between the two porins, its discovery is important as it was previously undetectable using traditional methods^{6,38}. Specific key residues in both porins, identified through the computational modelling methods described above (FIG. 4), were then evaluated for their role in carbapenem passage relative to the uptake of their natural substrates using a robust cell-based compound uptake assay. Finally, results from these studies led to the design of novel analogues with uptake mechanisms that were quite distinct from the parent compounds³⁶.

It is tempting to consider circumventing the challenges of compound penetration across bacterial membranes via the use of ‘Trojan horse’ strategies that ‘trick’ the bacteria into taking up antibiotics by conjugating them to moieties that are normally used to transport nutrients into the cells. Indeed, researchers have been intrigued for decades by a number of bioactive natural products with structural elements that mimic the natural substrates of peptide, sugar phosphate, nucleoside, polyamine and iron siderophore uptake pathways^{39,40}. Although there have been some efforts to exploit these uptake mechanisms to deliver inhibitors of cytoplasmic targets⁴¹, most have focused on molecules with ‘warheads’ that target cell wall synthesis by inhibiting penicillin binding proteins, which are located in the periplasm⁴². However, the appeal of this strategy is tempered by the strong potential for rapid induction or emergence of resistance, which is likely to be mediated through mutations in genes encoding the targeted transport mechanism. For example, one such compound had a sufficiently attractive antibacterial range, *in vitro* potency and chemical properties that it was advanced to Phase I clinical trials in 2010, but it has yet to progress further⁴³. This may be due to the lack of correlation between *in vitro* activity and *in vivo* efficacy that has been observed for this class of compounds by two independent research groups (A.M., manuscript in preparation, and REF. 44), which is attributed to a bacterial adaptation phenotype that occurs during infection but not under standard *in vitro* conditions of bacterial growth.

Another challenge faced by antibacterial researchers is the lack of a robust method to precisely and rapidly measure compound uptake by bacterial cells. This type of assay would greatly enable not only research into bacterial membrane penetration as described above but also inform the correlation of target inhibition to whole cell activity for a given series of inhibitors. Most existing techniques rely on either fluorescent⁴⁵ or radiometric⁴⁶ detection methods, or those based on liquid chromatography and mass spectrometry^{47,48} that require multiple wash steps and/or oil-based separation of cells from media. All of these approaches require both bacteria- and compound-specific optimization and none is amenable to higher throughput screening. However, recent advances in bioanalytical tools and their applications — for example single cell metabolomics based on mass spectrometry, microfluidics and capillary separations⁴⁹ — may aid in answering this problem in the near future.

Conclusions and next steps

Our analysis of antibacterial HTS programmes at AstraZeneca suggests that the outlook for identifying novel antibacterial agents might not be as bleak as previously considered. However, although many biochemical screens of genetically validated targets can clearly identify suitable chemical matter that warrants further investigation, there remains a substantial gap in the understanding of how to convert these hits into leads with cellular activity. The good news is that there are several efforts underway that may help to address this gap. These include the Innovative Medicines Initiative on Translocation⁵⁰, a 5-year, €30 million collaborative effort between the European Union, the European Federation of Pharmaceutical Industries and Associates (EFPIA) and Europe's leading academic scientists. This initiative aims to solve the riddle of how drugs enter Gram-negative bacteria using multiple workstreams, such as the assembly of a shared set of clinical isolates that cover a range of relevant membrane-permeability resistance mechanisms, the development and optimization of *in vitro* assays to better mimic envelope permeability at infection sites and omics approaches to characterize and quantify porin and efflux-pump changes that occur during infection. Greater understanding of the role of porins in drug permeation is also being gained through the determination of bacterial porin structures using X-ray crystallography, the use of molecular simulations to understand porin function and specificity, and the use of genetically regulated strains to determine or confirm the role of porins in permeation (including cells with point mutations in the porins to elucidate structural requirements for substrate recognition). All of these approaches have not been routinely available in the antibacterial discovery programmes carried out to date.

Initial results from our laboratories indicate that an approach that combines these new technologies in a concerted fashion is cause for a positive outlook on potential breakthroughs in understanding the uptake of other antibiotic classes. Ultimately, this may lead to new strategies that can be used to design more penetrant drugs in a coherent manner. The advent of these technologies — coupled with a new regulatory framework to simplify the development of pathogen-specific therapies³ and an improved funding landscape aided by government initiatives and open innovation models⁵¹ — may substantially enhance our ability to discover the novel antibacterial therapies that are desperately needed to address the threat of multidrug-resistant pathogens.

Ruben Tommasi and Alita A. Miller are at Entasis Therapeutics and Dean G. Brown is at AstraZeneca Pharmaceuticals, 35 Gatehouse Drive, Waltham, Massachusetts 02451, USA.

Grant K. Walkup is at Ajios Pharmaceuticals, 88 Sidney Street, Cambridge, Massachusetts 02139, USA.

John I. Manchester is at Novartis Institute for BioMedical Research, 186 Massachusetts Avenue, Cambridge, Massachusetts, USA.

Correspondence to: R. T.
e-mail: ruben.tommasi@entasisix.com

doi:10.1038/nrd4572

Published online 3 July 2015; corrected online 14 July & 14 August 2015

- World Health Organization. *Antimicrobial Resistance: Global Report on Surveillance* http://apps.who.int/iris/bitstream/10665/112642/1/9789241564748_eng.pdf?ua=1 (WHO 2014).
- Boucher, H. W. *et al.* 10 × '20 progress — development of new drugs active against Gram-negative Bacilli: an update from the Infectious Diseases Society of America. *Clin. Infect. Dis.* **56**, 1685–1694 (2013).
- Rex, J. H., Goldberger, M., Eisenstein, B. I. & Harney, C. The evolution of the regulatory framework for antibacterial agents. *Ann. NY Acad. Sci.* **1323**, 11–21 (2014).
- Payne, D. J., Gwynn, M. N., Holmes, D. J. & Pompliano, D. L. Drugs for bad bugs: confronting the challenges of antibacterial discovery. *Nat. Rev. Drug Discov.* **6**, 29–40 (2007).
- This paper provides an overview of the HTS efforts directed at the identification of novel antibacterials at GSK, which comprised the study of more than 300 genes and 70 high-throughput screens over a period of 7 years. Furthermore, a thorough analysis of potential reasons for failure is presented along with perspectives on how to improve the likelihood of success through focusing on broader chemical diversity.**
- O'Shea, R. & Moser, H. E. Physicochemical properties of antibacterial compounds: implications for drug discovery. *J. Med. Chem.* **51**, 2871–2878 (2008).
- Eren, E. *et al.* Substrate specificity within a family of outer membrane carboxylate channels. *PLoS Biol.* **10**, e1001242 (2012).
- de Jonge, B. L. *et al.* Discovery of inhibitors of 4'-phosphopantetheine adenylyltransferase (PPAT) to validate PPAT as a target for antibacterial therapy. *Antimicrob. Agents Chemother.* **57**, 6005–6015 (2013).
- Copeland, R. A. *Evaluation of Enzyme Inhibitors in Drug Discovery: A Guide for Medicinal Chemists and Pharmacologists*. 2nd edn (John Wiley & Sons, 2013).
- Roemer, T., Davies, J., Gaever, G. & Nislow, C. Bugs, drugs and chemical genomics. *Nat. Chem. Biol.* **8**, 46–56 (2012).
- Buurman, E. T. *et al.* *In vitro* validation of acetyltransferase activity of GImU as an antibacterial target in *Haemophilus influenzae*. *J. Biol. Chem.* **286**, 40734–40742 (2011).
- Mills, S. D. *et al.* Novel bacterial NAD⁺-dependent DNA ligase inhibitors with broad-spectrum activity and antibacterial efficacy *in vivo*. *Antimicrob. Agents Chemother.* **55**, 1088–1096 (2011).
- Lajiness, M. S., Maggiora, G. M. & Shanmugasundaram, V. Assessment of the consistency of medicinal chemists in reviewing sets of compounds. *J. Med. Chem.* **47**, 4891–4896 (2004).
- Sanguinetti, M. C. & Tristani-Firouzi, M. hERG potassium channels and cardiac arrhythmia. *Nature* **440**, 463–469 (2006).
- Seidler, J., McGovern, S. L., Doman, T. N. & Shoichet, B. K. Identification and prediction of promiscuous aggregating inhibitors among known drugs. *J. Med. Chem.* **46**, 4477–4486 (2003).
- Clinical and Laboratory Standards Institute. *CLSI document M07-A9: Methods for Dilution Antimicrobial Susceptibility Tests for Bacteria That Grow Aerobically; Approved Standard 9th edn* (CLSI, 2012).
- Uria-Nickelsen, M. *et al.* Novel topoisomerase inhibitors: microbiological characterisation and *in vivo* efficacy of pyrimidines. *Int. J. Antimicrob. Agents* **41**, 363–371 (2013).
- Keating, T. A. *et al.* *In vivo* validation of thymidylate kinase (TMK) with a rationally designed, selective antibacterial compound. *ACS Chem. Biol.* **7**, 1866–1872 (2012).
- Brown, D. G., May-Dracka, T. L., Gagnon, M. M. & Tommasi, R. Trends and exceptions of physical properties on antibacterial activity for Gram-positive and Gram-negative pathogens. *J. Med. Chem.* **57**, 10144–10161 (2014).
- Hann, M. M. Molecular obesity, potency and other additions in drug discovery. *Med. Chem. Commun.* **2**, 349–355 (2011).
- Leeson, P. D. & Springthorpe, B. The influence of drug-like concepts on decision-making in medicinal chemistry. *Nat. Rev. Drug Discov.* **6**, 881–890 (2007).
- Wenlock, M. C., Austin, R. P., Barton, P., Davis, A. M. & Leeson, P. D. A comparison of physicochemical property profiles of development and marketed oral drugs. *J. Med. Chem.* **46**, 1250–1256 (2003).
- Hernandez, V. *et al.* Discovery of a novel class of boron-based antibacterials with activity against Gram-negative bacteria. *Antimicrob. Agents Chemother.* **57**, 1394–1403 (2013).
- Rees, D. C., Congreve, M., Murray, C. W. & Carr, R. Fragment-based lead discovery. *Nat. Rev. Drug Discov.* **3**, 660–672 (2004).
- Ling, L. L. *et al.* A new antibiotic kills pathogens without detectable resistance. *Nature* **517**, 455–459 (2015).
- Brown, D. G., Lister, T. & May-Dracka, T. L. New natural products as new leads for antibacterial drug discovery. *Bioorg. Med. Chem. Lett.* **24**, 413–418 (2014).
- Cabeen, M. T. & Jacobs-Wagner, C. Bacterial cell shape. *Nat. Rev. Micro* **3**, 601–610 (2005).
- Silhavy, T. J., Kahne, D. & Walker, S. The bacterial cell envelope. *Cold Spring Harb. Perspect. Biol.* **2**, a000414 (2010).
- Denyer, S. P. & Maillard, J. Y. Cellular impermeability and uptake of biocides and antibiotics in Gram-negative bacteria. *J. Appl. Microbiol.* **92**, 35S–45S (2002).
- Hancock, R. E. & Brinkman, F. S. Function of pseudomonas porins in uptake and efflux. *Annu. Rev. Microbiol.* **56**, 17–38 (2002).
- Biswas, S., Mohammad, M. M., Patel, D. R., Movileanu, L. & van den Berg, B. Structural insight into OprD substrate specificity. *Nature Struct. Mol. Biol.* **14**, 1108–1109 (2007).
- This paper provides an encompassing structural and biophysical rationale for the adoption of the OccD and OccK nomenclature standard for *P. aeruginosa* outer-membrane carboxylate channels (porins). Additionally, it presents and summarizes the main methods that are presently at the forefront of studying porin dynamics and elucidating substrate selectivity: single-channel electrophysiology and radioactive-tracer direct measurement (or competition). The authors also demonstrate the selective binding and transport of antibiotics by these channels.**
- Ceccarelli, M., Vargiu, A. & Ruggerone, P. A kinetic Monte Carlo approach to investigate antibiotic translocation through bacterial porins. *J. Phys. Condens. Matter* **24**, 104012 (2012).
- Eren, E. *et al.* Toward understanding the outer membrane uptake of small molecules by *Pseudomonas aeruginosa*. *J. Biol. Chem.* **288**, 12042–12053 (2013).
- Kattner, C., Zaucha, J., Jaenecke, F., Zachariae, U. & Tanabe, M. Identification of a cation transport pathway in *Neisseria meningitidis* PorB. *Proteins* **81**, 830–840 (2013).
- Shaw, D. E. *et al.* Atomic-level characterization of the structural dynamics of proteins. *Science* **330**, 341–346 (2010).
- This paper describes a landmark 1-millisecond molecular-dynamics simulation of bovine pancreatic trypsin inhibitor (BPTI) as well as simulations of FIP35 and villin, which demonstrate that not only are long timescale simulations stable — a point which was previously in doubt — but they are also capable of accurately reproducing the experimentally observed behaviour of these systems, including the kinetics of protein folding to the native state, in addition to the detail these methods provide at atomic resolution.**
- Laio, A. Parrinello, M. Escaping free-energy minima. *Proc. Natl Acad. Sci. USA* **99**, 12562–12566 (2002).

36. Isabella, V. M. *et al.* Towards the rational design of carbapenem uptake in *Pseudomonas aeruginosa*. *Chem. Biol.* **22**, 535–547 (2015).
Using a multidisciplinary approach, including genetics, molecular dynamic simulations and medicinal chemistry, these authors discovered a novel mechanism of carbapenem uptake in *P. aeruginosa*, which led to the generation of novel carbapenems with altered uptake properties.
37. van Opijnen, T., Lazinski, D. W. & Camilli, A. Genome-wide fitness and genetic interactions determined by Tn-seq, a high-throughput massively parallel sequencing method for microorganisms. *Curr. Protoc. Microbiol.* **36**, 1E.3.1–1E.3.24 (2015).
This study describes Tn-seq, a newly developed genomic platform that deploys high-throughput next-generation sequencing on saturated transposon-insertion libraries of microorganisms to decipher complex fitness phenotypes on a global scale.
38. Tamber, S. & Hancock, R. E. W. Involvement of two related porins, OprD and OprP, in the uptake of arginine by *Pseudomonas aeruginosa*. *FEMS Microbiol. Lett.* **260**, 23–29 (2006).
39. Möllmann, U., Heinisch, L., Bauernfeind, A., Köhler, T. & Ankel-Fuchs, D. Siderophores as drug delivery agents: application of the “Trojan Horse” strategy. *Biomaterials* **22**, 615–624 (2009).
40. deCarvalho, C. C. & Fernandes, P. Siderophores as “Trojan Horses”: tackling multidrug resistance? *Frontiers Microbiol.* **5**, 290 (2014).
41. Rivault, F. *et al.* Synthesis of pyochelin–norfloxacin conjugates. *Bioorg. Med. Chem. Lett.* **17**, 640–644 (2007).
42. Page, M. G. P. Siderophore conjugates. *Ann. NY Acad. Sci.* **1277**, 115–126 (2013).
43. Page, M. G. P. *et al.* *In vitro* and *in vivo* properties of BAL30376, a β -lactam and dual β -lactamase inhibitor combination with enhanced activity against Gram-negative Bacilli that express multiple β -lactamases. *Antimicrob. Agents Chemother.* **55**, 1510–1519 (2011).
44. Tomaras, A. P. *et al.* Adaptation-based resistance to siderophore-conjugated antibacterial agents by *Pseudomonas aeruginosa*. *Antimicrob. Agents Chemother.* **57**, 4197–4207 (2013).
45. Ricci, V. & Piddock, L. Accumulation of garenoxacin by *Bacteroides fragilis* compared with that of five fluoroquinolones. *J. Antimicrob. Chemother.* **52**, 605–609 (2003).
46. Williams, K. J. & Piddock, L. J. Accumulation of rifampicin by *Escherichia coli* and *Staphylococcus aureus*. *J. Antimicrob. Chemother.* **42**, 597–603 (1998).
47. Bhat, J., Narayan, A., Venkatraman, J. & Chatterji, M. LC–MS based assay to measure intracellular compound levels in *Mycobacterium smegmatis*: linking compound levels to cellular potency. *J. Microbiol. Methods* **94**, 152–158 (2013).
48. Davis, T. D., Gerry, C. J. & Tan, D. S. General platform for systematic quantitative evaluation of small-molecule permeability in bacteria. *ACS Chem. Biol.* **9**, 2535–2544 (2014).
49. Rubakhin, S. S., Lanni, E. J. & Sweedler, J. V. Progress toward single cell metabolomics. *Curr. Opin. Biotechnol.* **24**, 95–104 (2013).
50. IMI. Translocation: molecular basis of the bacterial cell wall permeability. *Innovative Medicines Initiative* <http://www.imi.europa.eu/content/translocation> (2008).
51. May, M. Drug development: time for teamwork. *Nature* **509**, S4–S5 (2014).
52. Valentino, M. D. *et al.* Genes contributing to *Staphylococcus aureus* fitness in abscess- and infection-related ecologies. *mBio* **5**, e01729-14 (2014).
53. Subashchandrabose, S., Smith, S. N., Spurbeck, R. R., Kole, M. M. & Mobley, H. L. T. Genome-wide detection of fitness genes in uropathogenic *Escherichia coli* during systemic infection. *PLoS Pathog.* **9**, e1003788 (2013).
54. Palace, S. G., Proulx, M. K., Lu, S., Baker, R. E. & Goguen, J. D. Genome-wide mutant fitness profiling identifies nutritional requirements for optimal growth of *Yersinia pestis* in deep tissue. *mBio* **5**, e01385-14 (2014).
55. Wang, N., Ozer, E. A., Mandel, M. J. & Hauser, A. R. Genome-wide identification of *Acinetobacter baumannii* genes necessary for persistence in the lung. *mBio* **5**, e01163-14 (2014).
56. Skurnik, D. *et al.* Enhanced *in vivo* fitness of carbapenem-resistant *oprD* mutants of *Pseudomonas aeruginosa* revealed through high-throughput sequencing. *Proc. Natl Acad. Sci. USA* **110**, 20747–20752 (2013).
57. Turner, K. H., Everett, J., Trivedi, U., Rumbaugh, K. P. & Whiteley, M. Requirements for *Pseudomonas aeruginosa* acute burn and chronic surgical wound infection. *PLoS Genet.* **10**, e1004518 (2014).
58. Moule, M. G. *et al.* Genome-wide saturation mutagenesis of *Burkholderia pseudomallei* K96243 predicts essential genes and novel targets for antimicrobial development. *mBio* **5**, e00926-13 (2014).
59. Gallagher, L. A., Shendure, J. & Manoil, C. Genome-scale identification of resistance functions in *Pseudomonas aeruginosa* using Tn-seq. *mBio* **2**, e00315-10 (2011).
60. Cabot, G. *et al.* *Pseudomonas aeruginosa* ceftolozane-tazobactam resistance development requires multiple mutations leading to overexpression and structural modification of AmpC. *Antimicrob. Agents Chemother.* **58**, 3091–3099 (2014).
61. Jones, C. J. *et al.* ChIP-Seq and RNA-Seq reveal an AmrZ-mediated mechanism for cyclic di-GMP synthesis and biofilm development by *Pseudomonas aeruginosa*. *PLoS Pathog.* **10**, e1003984 (2014).
62. Hua, X., Chen, Q., Li, X. & Yu, Y. Global transcriptional response of *Acinetobacter baumannii* to a subinhibitory concentration of tigecycline. *Int. J. Antimicrob. Agents* **44**, 337–344 (2014).
63. Tan, S. Y.-Y. *et al.* Comparative systems biology analysis and mode of action of the isothiocyanate compound iberin on *Pseudomonas aeruginosa*. *Antimicrob. Agents Chemother.* **58**, 6648–6659 (2014).
64. Armengaud, J. Microbiology and proteomics, getting the best of both worlds! *Environ. Microbiol.* **15**, 12–23 (2013).
65. Chavali, A. K., D'Auria, K. M., Hewlett, E. L., Pearson, R. D. & Papin, J. A. A metabolic network approach for the identification and prioritization of antimicrobial drug targets. *Trends Microbiol.* **20**, 113–123 (2012).
66. Lebeis, S. L. & Kaiman, D. Aligning antimicrobial drug discovery with complex and redundant host-pathogen interactions. *Cell Host Microbe* **5**, 114–122 (2009).
67. Nayar, A. S. *et al.* Novel antibacterial targets and compounds revealed by a high-throughput cell wall reporter assay. *J. Bacteriol.* **197**, 1726–1734 (2015).

Acknowledgements

This review represents many years of hard work by former members of the AstraZeneca Infection Innovative Medicine and Early Development department, whom the authors would like to gratefully acknowledge for their intelligence, creativity and dedication to the advancement of this important field of research.

Competing interests statement

The authors declare [competing interests](#): see Web version for details.

FURTHER INFORMATION

Discuva website: <http://www.discuva.com>

DATABASES

RCSB Protein Data Bank:

<http://www.rcsb.org/pdb/home/home.do>

ALL LINKS ARE ACTIVE IN THE ONLINE PDF

ERRATUM

ESKAPEing the labyrinth of antibacterial discovery

Ruben Tommasi, Dean G. Brown, Grant K. Walkup, John I. Manchester and Alita A. Miller

Nature Reviews Drug Discovery **8**, 529–542 (2015)

In the legend of Figure 3, Gram-negative and Gram-positive bacteria were incorrectly labelled. This has been corrected in the online version of the article.